Research Article

Eman O. Hamed, Mohamed G. Assy, Nabil H. Ouf, Doaa A. Elsayed and Magda H. Abdellattif*

Cyclization of *N*-acetyl derivative: Novel synthesis – azoles and azines, antimicrobial activities, and computational studies

https://doi.org/10.1515/hc-2022-0004
received August 01, 2021; accepted October 19, 2021

Abstract: 2-Pyridone is considered as one of the most famous efficient pharmaceutical compounds. Many approaches were discovered to synthesize 2-pyridone. In this present research, chloroacetylation of benzylamine at simple conditions, EtONa/EtCOONa produced *N*-benzyl-2-chloroacetamide **2**. Compound **2** was allowed to react with different reagents. These reagents are acetylacetone, ethyl cyanoacetate, ethyl acetoacetate, and diethyl malonate, creating *2-pyridone derivatives* with a good yield. The structures of the prepared compounds were elucidated by spectral data (IR, ^{1}HNMR, and ^{13}CNMR). The synthesized compound was tested for its antimicrobial activity against the Gram-positive (*Staphylococcus aureus*) and the Gram-negative (*Escherichia coli*) bacteria. In addition, the antifungal activities of the compounds were tested against two fungi (*Candida albicans* and *Aspergillus flavus*). Molecular docking studies were applied using the Autodock vina method. Theoretical methods prove all the experimental results by using molecular docking using Autodock vina and by ADEMT studies. The docking results represent that compound **20** had the best docking free energy, and it is the effective compound toward the selected bacterial and fungal proteins. ADME studies showed that the only compound **18** could cross the blood–brain barrier, and compound **15** was predicted to be soluble.

Keywords: 2-pyridone, ethyl cyanoacetate, chloroacetamide, lactam–lactim tautomerism, molecular docking, ADMET

*** Corresponding author: Magda H. Abdellattif,** Department of Chemistry, College of Science, Taif University, Taif, 21944, Saudi Arabia, e-mail: m.hasan@tu.edu.sa
Eman O. Hamed, Nabil H. Ouf, Doaa A. Elsayed: Department of Chemistry, Faculty of Science, Zagazig University, Zagazig 44519, Egypt
Mohamed G. Assy: Department of Chemistry, Faculty of Science, Zagazig University, Zagazig 44519, Egypt, e-mail: dmgomaa59@gmail.com

1 Introduction

Cyclization of α-halogenacetamides is a building block for synthesizing several organic compounds, which attracted the attention of many researchers due to their importance in various fields [1–3]. While some derivatives occur naturally, 2-pyridone does not [4,5]. 2-Pyridone has two forms of tautomerism (keto and enol forms), expressed as lactam–lactim tautomerism. In this type of tautomerism, the H^{+} on the nitrogen atom can be attached to the oxygen atom to obtain the second tautomer. In the solid state, 2-pyridone exists in the keto form, where the IR analysis indicated the presence of the ketone group. However, in the solution state, 2-pyridone tautomerization depends on the polarity of the solvent, wherein polar solvents exist in ketone form, while nonpolar solvents present as the hydroxyl form [6]. The dimerization of 2-pyridone and 2-hydroxy pyridine underwent through hydrogen bond [7].

α-Pyridone derivatives have wide and important applications in many fields like industry, biology, and medicine. They are used as anticancer [8,9], anti-inflammatory [10,11], antimicrobial, antifungal [12–15], pharmaceutical [16], antiviral [17,18], anti-oxidant [19], dyes [20–24], fluorescents [25], and natural products [26,27]. In addition, 2-pyridone has catalytic activity, and hence, it can be used as a catalyst in proton-dependent reactions like aminolysis of esters [28–30] and its uses as a ligand in coordination chemistry [31,32]. Therefore, these animated researchers prepare 2-pyridone and its derivatives through cyclic and condensation of an acyclic system [33–40]. Thus, in this work, the preparation and properties of some 2-pyridone derivatives are presented. Computational studies involving molecular docking by auto dock vina were used to predict and prove the biological studies. ADMET studies indicated the prediction and validation of the activity of the synthesized compounds. The use of computational studies is one of the modern techniques that help describe the pharmacological properties of the

synthesized compounds. The consequence of the present research strengthens the applicability of these compounds as encouraging anticancer and antibacterial drugs that could help the medicinal chemists and pharmaceuticals further design and synthesize more effective drug candidates [41–44].

2 Results and discussion

2.1 Chemistry

Chloroacetylation of benzylamine furnished multifunction product 2 (Scheme 1). The stretching frequency of 2 was observed at 3,271, 1,641, and 1,546 cm^{-1} for N–H, C=O, and C=C, respectively. The exchangeable downfield signal of N–H was shown at 8.70 ppm. The synthetic strategy of producing a new pyridone system depends on the reaction of active methylene with 1 followed by intramolecular cyclization involving the condensation of the ester carbonyl with nucleophilic benzylic carbon in a basic medium. Thus, diethyl malonate underwent alkylation, cyclization followed by hydrolysis, subsequent CO_2 evolution, and enolization to furnish 6 (Scheme 1). IR spectrum led to peaks at 3,274, 1,644, and 1,549 for O–H, C=N, and C=C, respectively. O–H appeared at 13.2 and 15.14 ppm.

Acetyl acetone underwent alkylation by using 2 in a basic medium followed by cyclodehydration producing pyridone derivative 8. N–H, C=O, and C=C stretching frequency were observed at 3,275, 1,645, and 1,549 cm^{-1}, respectively. The N–H signal was detected at 11.09 ppm, and the carbonyl carbon signal was detected at 139.29 and 166.43.

Ethyl cyanoacetate underwent SN reaction with 2, cyclization, iminohydrolysis, dehydrogenation followed by ester hydrolysis, and subsequent decarboxylation leading to 12 (Scheme 2). IR spectrum led to C=O and C=N, while there is no N–H signal.

As depicted in Scheme 2, cyclo-condensation of 2 and ethyl acetoacetate furnished pyridone derivative 15. IR

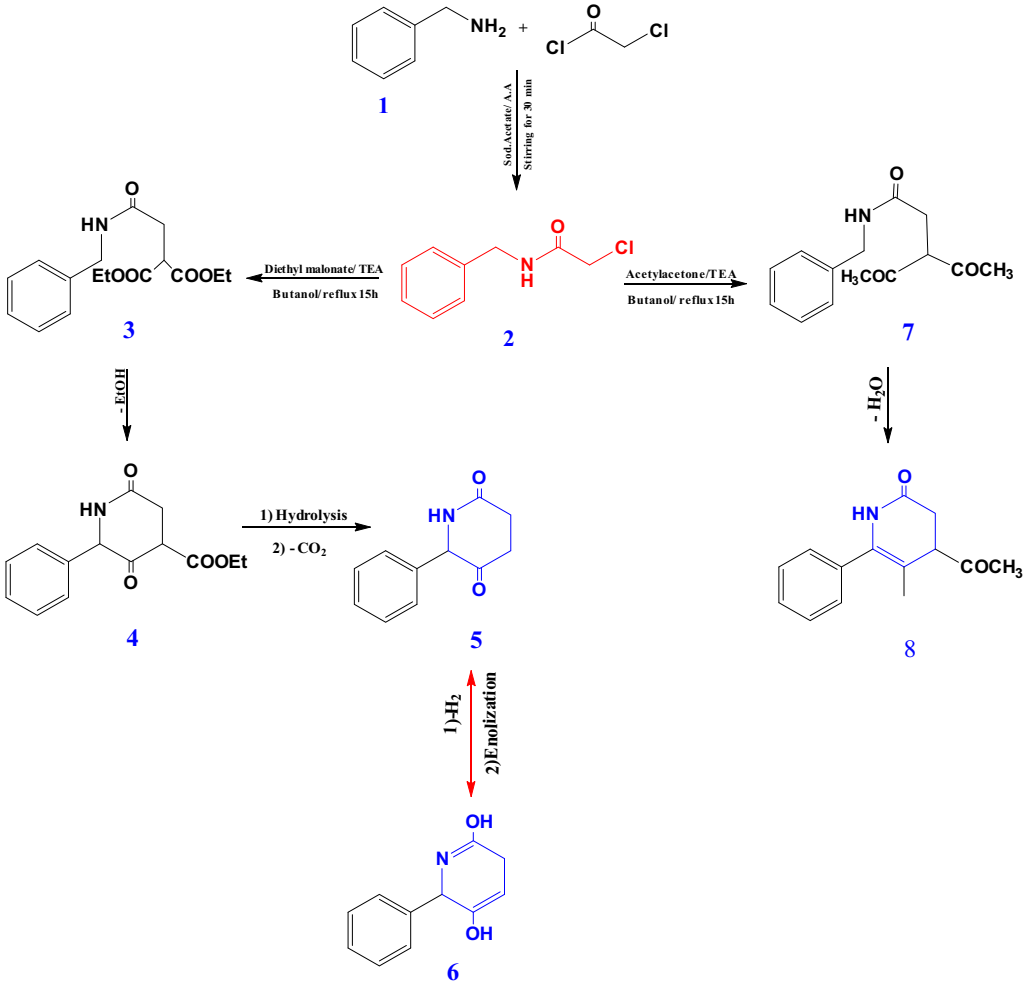

Scheme 1: Alkylation followed by cyclization of 2 with active methylene.

peaks presented at 3,275, 1,644, and 1,548 cm^{-1} due to O–H, C═N, and C═C, respectively. The O–H downfield signal was observed at 12.2 ppm. The imidazole cyclization 16 was observed by using thiourea as a cyclizing agent. IR spectrum showed peaks at 3,270, 1,641, and 1,311 for N–H, CN, and C═S, respectively. Intermolecular cyclization of 2 and benzaldehyde led to benzylic condensation followed by Michael's addition. IR spectrum led to N–H, C═O, and C═C function, the N–H signal was observed at 8.62 ppm, and carbonyl carbon was located at 134.01.

Subjecting 2 to added to heteroallene electrophilic carbon proved piperazine cyclization led to 20 (Scheme 3). N–H, CO, and C═S functions were observed at 3,272, 1,638, and 1,226 cm^{-1}, respectively. N–H signal was observed at 8.79 ppm.

2.2 Biology

The biological activity of the produced compounds was studied for their antimicrobial effects against the Gram-positive (*Staphylococcus aureus*) and the Gram-negative (*Escherichia coli*) bacteria. In addition, antifungal actions of the compounds were tested against two fungi (*Candida albicans* and *Aspergillus flavus*).

Table 1 shows that compounds **15**, **18**, and **20** have inhibitory effects on *S. aureus*, *E. coli*, *A. flavus*, *C. albicans* strains [41,42]. The antimicrobial activity of the tested compounds was determined using a modified Kirby-Bauer disc diffusion method [42].

Briefly, 100 µL of the test bacteria/fungi were grown in 10 mL of fresh media until they reached a count of approximately 108 cells/mL for bacteria 105 cells/mL for fungi [43].

2.3 Computational studies

2.3.1 Analyses of the docked complexes and ADME predictions

The information regarding the active site of the proteins was collected from the PDB database. Compound **8** showed the highest binding affinity with the DNA gyrase B of *S. aureus* with interaction was observed with Gly85,

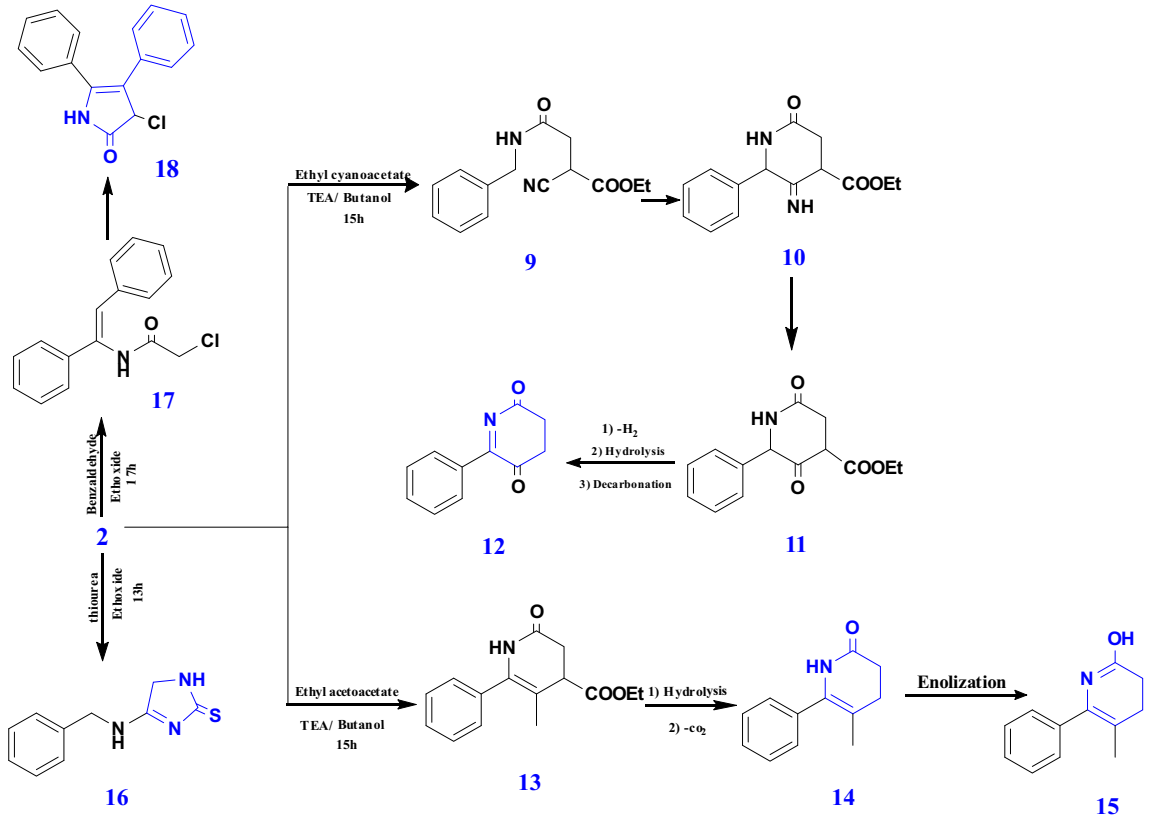

Scheme 2: Azole and azine generation from acylated product 2.

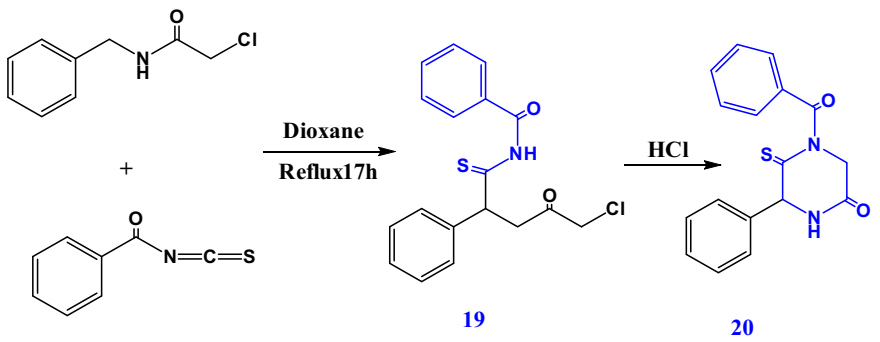

Scheme 3: Cyclization of compound **2** with benzoyl isothiocyanate.

Table 1: *In vitro* antibacterial and antifungal screening of the newly synthesized compounds

Sample	Inhibition zone diameter (mm/mg sample)			
	Bacterial species		Fungal species	
	G^+	G^-		
	Staphylococcus aureus	*Escherichia coli*	*Aspergillus flavus*	*Candida albicans*
Control: DMSO	0	0	0	0
6	0.0	0.0	0.0	0.0
8	9	0	0	0
15	10	12	0	0
18	10	10	0	0
20	11	15	10	26
Ampicillin Antibacterial agent	21	25	—	—
Amphotericin B Antifungal agent	—	—	17	21

Ile86, Ile51, and Ile175, while for *E. coli* DNA gyrase B, the compound **20** showed the highest free energy of binding with Asn46, Ile78, Pro79, and Ile90 were present in the binding cavity (Figure 1a and b). Similarly, compound **20** also has relatively higher interaction energy with urate oxide of *A. flavus* with residues Tyr30, Met32, Cys103, Hs104, and Trp106 in the docked site (Figure 1c). Furthermore, the compounds showed less binding affinity toward the glucosamine-6-phosphate synthase of *C. albicans*, with relatively higher energy for the docked complex of compound **20**, which was observed to have interacted with Leu411, Glu418, Tyr577, and Ala580 (Figure 1d). All the studied compounds demonstrated significant ADME properties, with the number of hydrogen bond donors [1,2], the number of hydrogen bond acceptors [2–5], and molecular weight of <320, which are considerable (Table 2). None of the studied compounds showed the ability to cross the blood–brain barrier except compound **18**, with the nontoxic nature of the selected compounds. Compound **15** was predicted to be soluble, with the rest of the compounds showing moderate solubility in water. All the designed compounds are practicality synthesizable, which can be indicated from the reasonable ranges presented through the ADME calculations.

3 Experimental and methodology

3.1 Chemistry

An electro-thermal IA 9100 apparatus was used for measuring melting points. Drying solvents were used for all experiments. Purification of the produced compounds was carried out by crystallization. The IR analyses (KBr disc) were performed using a Pye Unicom Sp-3-300 or a Shimadzu FTIR 8101 PC infrared spectrophotometer. The ^{1}HNMR and ^{13}CNMR spectra were recorded on Varian Mercury VX-300 NMR 500 (75.4) MHz at a spectrophotometer using DMSOd6 as a solvent. TMS was used as an internal reference for all chemical shifts expressed on the

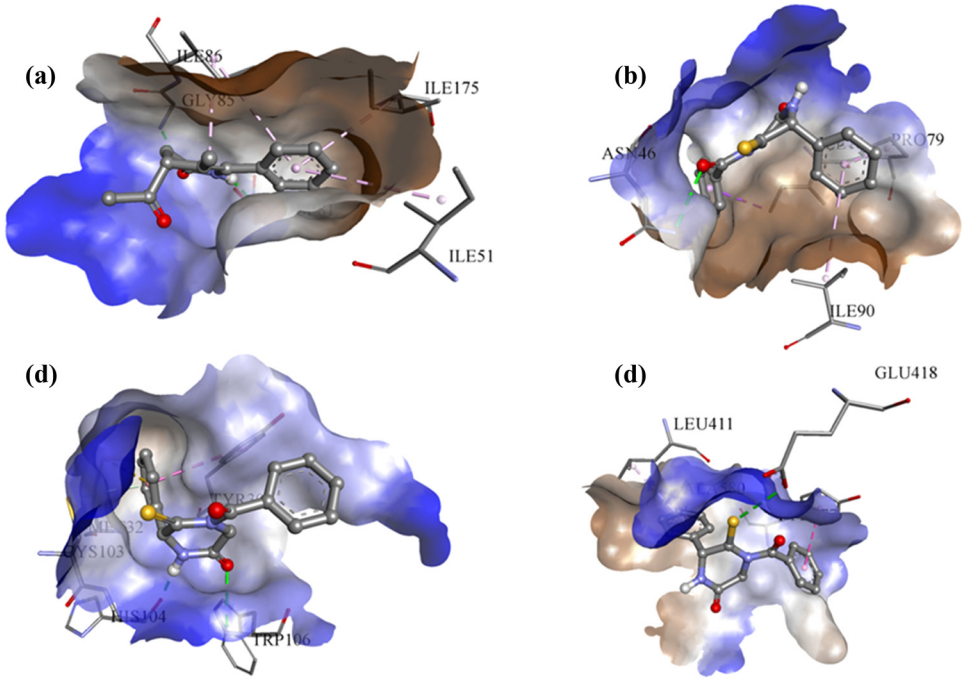

Figure 1: The docked complex formation (a) between *S. aureus* DNA gyrase B and compound **8**, (b) between *E. coli* DNA gyrase B and compound **20**, (c) between *A. flavus* urate oxide and compound **20**, and (d) between *C. albicans* glucosamine-6-phosphate synthase and compound **20**.

δ (ppm) scale. The values of the coupling constant (J) are given in Hz [45,46].

3.1.1 6-Phenyl-3,6-dihydropyridine-2,5-diol (6)

A solution of *N*-benzyl-2-chloroacetamide **2** (1,500 mg, 8 mmol), diethyl malonate (1.22 mL, 8 mmol), and TEA (1 mL) in butanol (20 mL) was refluxed for 15 h and then concentrated, and the formed precipitate was filtered off, washed with water, dried, and crystallized with a mixture of ethanol + H_2O by ratio of 1:3 to obtain white crystals of **6.** Yield 1175.1 mg (76%), m.p. 82–84°C. IR (KBr, ν, cm^{-1}): 3,274(2O–H) 1,644(C═N), 1,549(C═C). ^1H NMR (500 MHz, DMSO-*d*6) δ 7.42–7.27 (m, 5H), 5.87 (td, J = 5.8, 1.8 Hz, 1H), 5.15 (dt, J = 1.8, 0.9 Hz, 1H), 3.11–2.98 (m, 2H). ^{13}C NMR (125 MHz, chloroform-*d*) δ 172.57, 158.29, 138.62, 128.43, 127.58, 126.55, 97.57, 59.28, 26.34. Elemental analysis calculated (%) for $C_{11}H_{11}NO_2$ (189): C 69.83; H 5.86; N 7.40. Found: C 69.65; H 5.76; N 7.32.

3.1.2 4-Acetyl-5-methyl-6-phenyl-3,4-dihydropyridin-2(1*H*)-one (8)

A mixture of *N*-benzyl-2-chloroacetamide **2** (7,340 mg, 40 mmol), acetyl acetone (4.1 mL, 40 mmol), and TEA (1 mL) was refluxed in butanol (20 mL) for 15 h and then concentrated. The formed precipitate was filtered off, washed with water, dried, and recrystallized with mixture of ethanol + H_2O by ratio 1:3 to give brown powder of **8.** Yield 6,598 mg (72%), m.p. 80–86°C. IR (KBr, ν, cm^{-1}):

Table 2: List ADMET properties calculated for the selected inhibitors

S. no.	Compound name	QP log P_o/w	QPP Caco	QP log BB	QPPMDCK	#metab	QP log Khsa	Percent human oral absorption
1	**6**	2.42	205.83	−0.422	113.96	4	−0.235	82.535
2	**8**	1.83	1063.07	−0.402	528.52	3	−0.151	92.02
3	**15**	3.37	493.71	−0.119	293.40	3	0.085	94.92
4	**18**	2.92	597.64	0.466	606.98	2	0.301	93.75
5	**20**	2.40	351.05	−0.366	794.06	3	−0.089	86.60

Predicted 1: octanol/water partition coefficient; 2: Caco-2 cell permeability (nm/s); 3: brain/blood partition coefficient; 4: apparent MDCK cell permeability (nm/s); 5: human serum albumin binding; 6: number of metabolic reactions; 7: percent human oral absorption.

3,275(N–H), 1,645(C=O), 1,549(C=C). ^{1}H NMR (500 MHz, DMSO-*d*6) δ 7.55–7.47 (m, 3H), 7.43–7.36 (m, 2H), 4.70 (tdt, J = 7.7, 2.9, 1.5 Hz, 1H), 2.74 (dd, J = 15.7, 7.8 Hz, 1H), 2.52–2.46 (m, 1H), 2.13 (d, J = 1.5 Hz, 3H), 1.82 (d, J = 1.3 Hz, 3H). ^{13}C NMR (125 MHz, chloroform-*d*) δ 206.16, 171.14, 137.14, 133.68, 128.84, 128.20, 127.51, 114.39, 52.84, 37.35, 29.09, 16.52.

Elemental analysis calculated (%) for $C_{14}H_{15}NO_2$ (229.11): C 73.34; H 6.59; N 6.11. Found: C 73.29; H 6.46; N 6.6.

3.1.3 6-Phenyl-3,4-dihydropyridine-2,5-dione (12)

A solution of *N*-benzyl-2-chloroacetamide **2** (1,500 mg, 8 mmol), ethyl cyanoacetate (0.9 mL, 8 m.mol), and TEA (1 mL) in butanol (15 mL) was refluxed for 15 h and then concentrated. The formed precipitate was filtered off, washed with water, dried, and crystallized from butanol to give orange crystals of **12.** Yield 1112.8 mg (72%), m.p. 75–78°C. IR (KBr, ν, cm^{-1}): 1,641(C=O), 1,529(C=N). ^{1}H NMR (500 MHz, DMSO-d_6) δ 8.19–8.11 (m, 1H), 7.57–7.47 (m, 1H), 3.16–3.09 (m, 1H), 3.02–2.95 (m, 1H). ^{13}C NMR (125 MHz, chloroform-*d*) δ 193.68, 176.82, 162.36, 135.84, 130.19, 129.74, 129.31, 32.30, 31.61. Elemental analysis calculated (%) for $C_{11}H_9NO_2$ (187): C 70.58; H 4.85; N 7.48. Found: C 70.50; H 4.78; N 7.40.

3.1.4 5-Methyl-6-phenyl-3,4-dihydropyridin-2-ol (15)

A solution of *N*-benzyl-2-chloroacetamide **2** (1,000 mg, 5 mmol), ethyl acetoacetate (0.688 mL, 5 mmol), and TEA (1 mL) in butanol (20 mL) was refluxed for 15 h and then concentrated. The formed precipitate was filtered off, washed with water, dried, and crystallized from butanol to give pale yellow crystals of **15**. Yield 795.3 mg (78%), m.p. 79–80°C. IR (KBr, ν, cm^{-1}): 3,275(O–H), 1,644(C=N), 1,548(C=C). ^{1}H NMR (500 MHz, DMSO-d_6) δ 7.76–7.70 (m, 1H), 7.55–7.43 (m, 1H), 2.63–2.51 (m, 1H), 1.76 (s, 1H). ^{13}C NMR (125 MHz, chloroform-*d*) δ 167.90, 147.09, 137.19, 129.73, 128.22, 127.15, 126.12, 30.42, 26.15, 18.90. Elemental analysis calculated (%) for $C_{12}H_{13}NO$ (187.1): C 76.98; H 7.00; N 7.48. Found: 76.90; H 6.94; N 7.40.

3.1.5 4-(Benzyl amino)-1,5-dihydro-2*H*-imidazole-2-thione (16)

A solution of thiourea (380 mg, 5 mmol), *N*-benzyl-2-chloroacetamide **2** (1,000 mg, 5 mmol), and sodium (120 mg, 5 mmol) in ethanol (20 mL) was refluxed for 13 h, and then HCl was added dropwise till complete precipitate was obtained. The formed precipitate was filtered off, washed with water, dried, and crystallized from ethanol to give white crystals of **16.** Yield 860.5 mg (77%), m.p. 150–152°C. IR (KBr, ν, cm^{-1}): 3,270(N–H), 1,641(C=N), 1,311(C=S). ^{1}H NMR (500 MHz, DMSO-d_6) δ 9.40 (t, J = 5.0 Hz, 1H), 8.52 (t, J = 4.5 Hz, 1H), 7.36–7.30 (m, 1H), 7.31 (s, 3H), 7.34–7.22 (m, 2H), 4.52 (dd, J = 5.0, 0.8 Hz, 2H), 4.26 (d, J = 4.6 Hz, 2H). ^{13}C NMR (125 MHz, chloroform-*d*) δ 188.12, 167.22, 138.11, 128.29, 127.59, 127.49, 47.53, 46.85. Elemental analysis calculated (%) for $C_{10}H_{11}N_3S$ (205): C 58.51; H 5.40; N 20.47; S 15.62. Found: C 58.49; H 5.32; N 20.42; S 15.58.

3.1.6 3-Chloro-4,5-diphenyl-1,3-dihydro-2*H*-pyrrol-2-one (18)

A solution of benzaldehyde (0.54 mL, 5 mmol), *N*-benzyl-2-chloroacetamide **2** (1,000 mg, 5 mmol), and sodium (120 mg, 5 mmol) in ethanol (20 mL) was refluxed for 17 h, and then HCl was added dropwise till complete precipitate was obtained. The formed precipitate was filtered off, washed with water, dried, and crystallized from ethanol to give yellow crystals of **18.** Yield 1,099 mg (75%), m.p. 72–75°C. IR (KBr, ν, cm^{-1}): 3,283(N–H), 1,652(C=O), 1,532(C=C). ^{1}H NMR (500 MHz, DMSO-d_6) δ 9.28 (s, 1H), 7.60–7.54 (m, 2H), 7.53–7.46 (m, 1H), 7.44–7.34 (m, 4H), 7.34–7.26 (m, 3H), 6.14 (s, 1H). ^{13}C NMR (125 MHz, chloroform-*d*) δ 169.86, 135.75, 131.13, 130.22, 128.92, 128.58, 128.10, 128.00, 127.62, 126.32, 108.92, 57.22. Elemental analysis calculated (%) for $C_{16}H_{12}ClNO$ (269): C 71.25; H 4.48; Cl 13.14; N 5.19. Found: C 71.20; H 4.42; Cl 13.08; N 5.07.

3.1.7 4-Benzoyl-6-phenyl-5-thioxopiperazin-2-one (20)

A solution of benzoyl isothiocyanate (40 mmol), *N*-benzyl-2-chloroacetamide **2** (7,340 mg, 40 mmol) in dioxane (23 mL) was refluxed for 17 h and then poured into crushed ice. The formed precipitate was filtered off, washed with water, dried, and crystallized from dioxane to give pale orange crystals of **20.** Yield 8,680 mg (70%), m.p. 80–81°C. IR (KBr, ν, cm^{-1}): 3,272(N–H), 1,638(C=O), 1,552(C=C), 1,226(C=S). ^{1}H NMR (500 MHz, DMSO-d_6) δ 7.88–7.82 (m, 2H), 7.58–7.46 (m, 3H), 7.45–7.38 (m, 2H), 7.38–7.27 (m, 3H), 7.20 (d, J = 7.5 Hz, 1H), 5.64 (dd, J = 7.6, 0.7 Hz, 1H), 4.81–4.70 (m, 2H). ^{13}C NMR (125 MHz, chloroform-*d*) δ 200.42, 169.86, 166.14, 138.09, 135.23, 132.07,

129.12, 128.71, 128.04, 127.98, 62.79, 49.38. Elemental analysis calculated (%) for $C_{17}H_{14}N_2O_2S$ (310): C 65.79; H 4.55; N 9.03; S 10.33. Found: C 65.72; H 4.50; N 8.99; S 10.28.

3.2 Biology

A panel of Gram-positive bacteria (*Staphylococcus aureus*) and Gram-negative bacteria were examined for the antimicrobial action of the synthesized samples (*Escherichia coli*). The antifungal activities of the compounds were tested against two fungi (*Candida albicans* and *Aspergillus flavus*). Each sample was dissolved in DMSO, and 1 mg/mL of solutions were prepared separately as paper discs of Whitman filter paper of the standard size (5 cm) and were cut and sterilized in an autoclave. Petri dishes with nutrient agar media (agar 20 g + beef extract 3 g + peptone 5 g) were seeded with *Staphylococcus aureus*, *E. coli*, *Candida albicans*, and *Aspergillus flavus*, and the paper discs soaked in the desired concentration of the complex solution were placed aseptically. The Petri dishes were incubated at 36°C, and the inhibition zones were recorded after 24 h of incubation. Each test was repeated three times at the same solvents and solution concentration, and the antibacterial activities of a common standard antibiotic ampicillin and antifungal colitrimazole were recorded by using the same procedure as mentioned earlier. The percent activity index for the complex was calculated by the following formula:

$$\% \text{ Activity index} = \frac{\text{Zone of inhibition by test compound (diametre)}}{\text{Zone of inhibition by standard (diametre)}} \times 100.$$

3.3 Computational studies

3.3.1 Molecular docking and ADME analyses

As per the reference of the standard compounds used for the evaluation of the activities of the designed compounds, the protein target for each organism was selected from the Protein Data Bank (PDB) listed in Table 3. To study the effect of the drugs on bacterial protein, the DNA gyrase B (PDB IDs – 3U2K, 1KZN) was selected, but for *A. flavus*, it was urate oxide (PDB ID – 1R51), and for *C. albicans*, the glucosamine-6-phosphate synthase (PDB ID – 2PUV) was used. The selected structures were optimized using the utilities JAGUAR modules [42] present in MAESTRO (Schrödinger Release 2018-1: Maestro, Schrödinger, LLC, New York, NY, 2018). Consequently, molecular docking was performed between the designed molecules and target proteins using Autodock vina [43]. The best-docked conformations were statistically characterized through the combination of the free energy functional, the Lamarckian Genetic Algorithm, and the empirical force field [2]. The space of grid dimensional was set for 40 × 40 × 40 Å along the *XYZ* directions with varied central coordinates, and the maximum efficiency range was used in the parameters for the optimum results.

Furthermore, the ADME properties for each compound were calculated using QikProp tools present in the Schrodinger 2020-2. ADME (absorption, distribution, metabolism, and excretion), including drug-likeness analysis, is essential in the drug discovery, which accommodates to make a reasonable decisiveness on whether inhibitors can be conducted to a biological system [40,41]. A potent antagonistic interaction of inhibitors with a receptor protein or enzyme cannot guarantee the ability of an inhibitor as a drug; therefore, ADME assessment is essential in the drug development. Inhibitors with lower ADME properties and high toxicity effects on the biological systems are often the dominant explanation of most failed medicines in the clinical phase of experiments. From the output of some ADME and drug-likeness properties presented in Table 2, it was observed that most compounds have one or two violations of Lipinski's rule.

Table 3: List of molecular docking-based generated free energies of binding for the designed inhibitors

S. no.	Compound	Free energy of binding (kcal/mol)			
		S. aureus DNA gyrase B	*E. coli* DNA gyrase B	*A. flavus* Urate oxide	*C. albicans* Glucosamine-6-phosphate synthase
1.	**6**	−6.9	−6.6	−6.7	−6.0
2.	**8**	*−8.2*	−7.5	−7.7	−6.6
3.	**15**	−7.7	−7.2	−6.9	−5.9
4.	**18**	−7.5	−6.8	−7.4	−6.6
5.	**20**	−7.7	*−7.6*	*−8.2*	*−6.9*

4 Conclusion

α-Chloroacetyl derivative **2** underwent alkylation followed by intramolecular cyclization using carbonyl to provide pyridones. Target **2** underwent heterocyclization with benzaldehyde and benzoyl isothiocyanate to yield derivatives of 2-pyridone. The synthesized compound was tested for its antimicrobial activity against the Gram-positive (*Staphylococcus aureus*) and the Gram-negative (*Escherichia coli*) bacteria. The antifungal activities of the compounds were tested against two fungi (*Candida albicans* and *Aspergillus flavus*). Compound **20** has the highest antibacterial activity against Gram-positive (*Staphylococcus aureus*) and Gram-negative (*Escherichia coli*) bacteria and antifungal activity against *Candida albicans*. Such compounds that had antimicrobial activity should be further reused for the inhibitory microbial growth. The docking results show that compound **2** had the best docking free energy results toward *S. aureus*, while compound **20** was the effective compound toward the selected bacterial and fungal proteins. These results agreed with the experimental results.

Acknowledgements: The authors are very thankful to all the associated personnel in any reference that contributed to/for this research. M.H.A. is especially thankful to Taif University Researcher's Supporting Project Number (TURSP-2020/91), Taif University, Taif, Saudi Arabia.

Funding information: The authors state no funding involved.

Conflict of interest: The authors state no conflict of interest.

Data availability statement: The datasets generated during and/or analyzed during the current study are available from the corresponding author on reasonable request.

References

[1] Yuan C, Zhang H, Yuan M, Xie L, Cao X. Synthesis of 1, 4-diazepinone derivatives via a domino aza-Michael/SN 2 cyclization of 1-azadienes with α-halogenoacetamides. Org Biomol Chem. 2020;18(6):1082–6.

[2] Jin Q, Zhang D, Zhang J. Facile synthesis of 1, 2, 4, 5-tetrahydro-1, 4-benzodiazepin-3-ones via cyclization of N-alkoxy α-halogenoacetamides with N-(2-chloromethyl) aryl amides. Org Biomol Chem. 2019;17(45):9708–11.

[3] Fantinati A, Zanirato V, Marchetti P, Trapella C. The fascinating chemistry of α-haloamides. ChemistryOpen. 2020;9:100–70.

[4] Zhou C, Ni J, Zhang D, Sun C. Cellulosic adsorbent functionalized with macrocyclic pyridone pentamer for selectively removing metal cations from aqueous solutions. Carbohydr Polym. 2019;217:1–5.

[5] Christoforow A, Wilke J, Binici A, Pahl A, Ostermann C, Sievers S, et al. Design, synthesis, and phenotypic profiling of pyrano-furo-pyridone pseudo natural products. Angew Chem Int Ed. 2019;58(41):14715–23.

[6] Kulangiappar K, Anbukulandainathan M, Raju T. Synthetic communications: an international journal for rapid communication of synthetic organic chemistry. Synth Commun. 2014;1(44):2494–502.

[7] Szyc Ł, Guo J, Yang M, Dreyer J, Tolstoy PM, Nibbering ET, et al. The hydrogen-bonded 2-pyridone dimer model system. 1. Combined NMR and FT-IR spectroscopy study. J Phys Chem A. 2010;114(29):7749–60.

[8] Xie W, Wu Y, Zhang J, Mei Q, Zhang Y, Zhu N, et al. design, synthesis and biological evaluations of novel pyridone-thiazole hybrid molecules as antitumor agents. Eur J Med Chem. 2018;145:35–40.

[9] Li L-N, Wang L, Cheng YN, Cao ZQ, Zhang XK, Guo XL. Discovery and characterization of 4-hydroxy-2-pyridone derivative sambutoxin as a potent and promising anticancer drug candidate: activity and molecular mechanism. Mol Pharmaceutics. 2018;15(11):4898–911.

[10] Bai H, Sun R, Chen X, Yang L, Huang C. Microwave-assisted, solvent-free, three-component domino protocol: efficient synthesis of polysubstituted-2-pyridone derivatives. ChemistrySelect. 2018;3(17):4635–8.

[11] Gonçalves DS, de S Melo SM, Jacomini AP, J V da Silva M, Pianoski KE, Ames FQ, et al. Synthesis of novel 3, 5, 6-trisubstituted 2-pyridone derivatives and evaluation for their anti-inflammatory activity. Bioorg Med Chem. 2020;28(12):115549.

[12] Mahmoud MR, Abu El-Azm FSM, Ali AT, Ali YM. Synthesis and antimicrobial evaluation of some novel dithiolane, thiophene, coumarin, and 2-pyridone derivatives. Synth Commun. 2017;47(17):1591–600.

[13] Pandit AB, Savant MM, Ladva KD. An efficient one-pot synthesis of highly substituted pyridone derivatives and their antimicrobial and antifungal activity. J Heterocycl Chem. 2018;55(4):983–7.

[14] Ibrahim M. One-pot synthesis, characterization and antimicrobial activity of new 3-cyano-4-alkyl-6-(2, 5-dichlorothiophen-3-yl)-2 (1H)-pyridones. Jordan J Chem (JJC). 2015;10(2):98–107.

[15] Gaffer H, Elapasery M, Abbas D, Allam E. Synthesis of some new aryl-azo derivatives clubbed with pyridone and evaluating their biological broadcast. Egypt J Chem. 2020;63(3):1087–99.

[16] Maeng CY et al. Pharmaceutical composition comprising pyridone derivatives. Google Pat; 2018.

[17] Azzam RA, Elboshi HA, Elgemeie GH. Novel synthesis and antiviral evaluation of new benzothiazole-bearing N-sulfonamide 2-pyridone derivatives as USP7 enzyme inhibitors. ACS Omega. 2020;5(46):30023–36.

[18] Biswas A, Maity S, Pan S, Samanta R. Transition metal-catalysed direct C–H bond functionalizations of 2-pyridone beyond C3-selectivity. Chemistry – Asian J. 2020;15(14):2092–109.

[19] Chand K, Alsoghier HM, Chaves S, Santos MA. Tacrine-(hydroxybenzoyl-pyridone) hybrids as potential multifunctional anti-Alzheimer's agents: AChE inhibition, antioxidant activity and metal chelating capacity. J Inorg Biochem. 2016;163:266–77.
[20] Sun C, Huang Z, Wang J, Rao L, Zhang J, Yu J, et al. Modification of microcrystalline cellulose with pyridone derivatives for removal of cationic dyes from aqueous solutions. Cellulose. 2016;23(5):2917–27.
[21] Elapasery M, Shakra S, Abbas D, Gaffer HE, Allam EA. Synthesis of some azo disperse dyes based on pyridone moiety and their application on polyester fabrics. Egyptian J Chem. 2017;60(Conference Issue (The 8th International Conference of The Textile Research Division (ICTRD 2017), National Research Centre, Cairo 12622, Egypt.):97–102.
[22] Mijin D, et al. synthesis, solvatochromism, and biological activity of novel azo dyes bearing 2-pyridone and benzimidazole moieties. Turkish J Chem. 2018;42(3):896–907.
[23] Zhao X-L, Qian H-F, Huang W. Construction of benzothiazole/pyridone based bi-heterocyclic dyes and their NiII and CuII complexes. Dye Pigment. 2018;149:796–803.
[24] Al-Etaibi AM, El-Apasery MA. A comprehensive review on the synthesis and versatile applications of biologically active pyridone-based disperse dyes. Int J Environ Res Public Health. 2020;17(13):4714.
[25] Kadam ML, D, Patil, Sekar N. Fluorescent carbazole based pyridone dyes–synthesis, solvatochromism, linear and nonlinear optical properties. Opt Mater. 2018;85:308–18.
[26] Jessen HJ, Gademann K. 4-Hydroxy-2-pyridone alkaloids: structures and synthetic approaches. Nat product Rep. 2010;27(8):1168–85.
[27] Jessen HJ, Schumacher A, Schmid F, Pfaltz A, Gademann K. Catalytic enantioselective total synthesis of (+)-torrubiellone C. Org Lett. 2011;13(16):4368–70.
[28] Fischer CB, Steininger H, Stephenson DS, Zipse H. Catalysis of aminolysis of p-nitrophenyl acetate by 2-pyridones. J Phys Org Chem. 2005;18(9):901–7.
[29] Wang LH, Zipse H. Bifunctional catalysis of ester aminolysis–a computational and experimental study. Liebigs Annalen. 1996;1996(10):1501–9.
[30] Fischer CB, Polborn K, Steininger H, Zipse H. Synthesis and solid-state structures of alkyl-substituted 3-cyano-2-pyridones. Z Naturforschung B. 2004;59(10):1121–31.
[31] Donets PA, Cramer N. Ligand-controlled regiodivergent nickel-catalyzed annulation of pyridones. Angew Chem. 2015;127(2):643–7.
[32] Wang P, Verma P, Xia G, Shi J, Qiao JX, Tao S, et al. Ligand-accelerated non-directed C–H functionalization of arenes. Nature. 2017;551(7681):489–93.
[33] Poomathi N, Perumal P, Ramakrishna S. An efficient and eco-friendly synthesis of 2-pyridones and functionalized azaxanthone frameworks via indium triflate catalyzed domino reaction. Green Chem. 2017;19(11):2524–9.
[34] Torres M, Gil S, Parra M. New synthetic methods to 2-pyridone rings. Curr Org Chem. 2005;9(17):1757–79.
[35] Heravi MM, Hamidi H. Recent advances in synthesis of 2-pyridones: a key heterocycle is revisited. J Iran Chem Soc. 2013;10(2):265–73.
[36] Samzadeh-Kermani A. Heteropolyacid-catalyzed one-pot synthesis of 2-pyridone derivatives. Synlett. 2016;27(03):461–4.
[37] Babaee S, Zarei M, Sepehrmansourie H, Zolfigol MA, Rostamnia S. Synthesis of metal–organic frameworks MIL-101 (Cr)-NH2 containing phosphorous acid functional groups: Application for the synthesis of N-Amino-2-pyridone and pyrano [2, 3-c] pyrazole derivatives via a cooperative vinylogous anomeric-based oxidation. ACS Omega. 2020;5(12):6240–9.
[38] Jia H, Song Y, Yu J, Zhan P, Rai D, Liang X, et al. design, synthesis and primary biological evaluation of the novel 2-pyridone derivatives as potent non-nucleoside HBV inhibitors. Eur J Med Chem. 2017;136:144–53.
[39] Abdellattif MH, Abdel-Rahman A, Arief M, Mouneir SM, Ali A, Hussien MA, et al. Novel 2-Hydroselenonicotinonitriles and Selenopheno[2, 3-b]pyridines: Efficient Synthesis, Molecular Docking-DFT Modeling, and Antimicrobial Assessment. Front Chem. May 2021;9:10. doi: 10.3389/fchem.2021.672503.
[40] Rai SK, Khanam S, Khanna RS, Tewari AK. Design and synthesis of 2-pyridone based flexible dimers and their conformational study through X-ray diffraction and density functional theory: perspective of cyclooxygenase-2 inhibition. Cryst Growth Des. 2015;15(3):1430–9.
[41] Amer MMK, Aziz MA, Shehab WS, Abdellattif MH, Mouneir SM. Recent advances in chemistry and pharmacological aspects of 2-pyridone scaffolds. J Saudichemical Soc. 2021;25(6):101259. doi: 10.1016/ j.jscs.2021.101259.
[42] Abdellattif MH, Shahbaaz M, Arief MMH, Hussien MA. Oxazinethione derivatives as a precursor to pyrazolone and pyrimidine derivatives: Synthesis, biological activities, molecular modeling, ADME, and molecular dynamics studies. Molecules. 2021;26:5482. doi: 10.3390/molecules26185482.
[43] Ochevarov AD, Harder E, Hughes TF, Greenwood JR, Braden DA, Philipp DM, et al. A high-performance quantum chemistry software program with strengths in life and materials sciences. Int J Quant Chem. 2013;113:2110–42. doi: 10.1002/qua.24481.
[44] Trott O, Olson AJ. AutoDock Vina: improving the speed and accuracy of docking with a new scoring function, efficient optimization and multithreading. J Comput Chem. 2010;31:455–61. doi: 10.1002/jcc.21334.
[45] Zhou L, Dai S, Xu S, She Y, Li Y, Leveneur S, et al. Piezoelectric effect synergistically enhances the performance of Ti32-oxo cluster/BaTiO3/CuS p-n heterojunction photocatalytic degradation of pollutants. Ind Chem React Eng. 2021;291:120019. doi: 10.1016/j.apcatb.2021.120019.
[46] Xu S, Zhu Q, Xu S, Yuan M, Lin X, Lin W, et al. The phase behavior of n-ethylpyridinium tetrafluoroborate and sodium-based salts ATPS and its application in 2-chlorophenol extraction. Chin J Chem Eng. May 2021;33:76–82. doi: 10.1016/j.cjche.2020.07.024.